Int. J. Solids Structures Vol. 23, No. 1, pp. 133–151, 1987
Printed in Great Britain.

0020–7683/87 $3.00 + .00
Pergamon Journals Ltd.

ENDOCHRONIC PLASTICITY: SOME BASIC PROPERTIES OF PLASTIC FLOW AND FAILURE

H. MURAKAMI† and H. E. READ
S-CUBED, A Division of Maxwell Laboratories, La Jolla, CA 92038-1620, U.S.A.

(*Received* 25 *July* 1985; *in revised form* 21 *February* 1986)

Abstract—Some basic properties of plastic flow of the new endochronic plasticity theory are established, using analytical and numerical methods. Particular attention is given to the case, of significant practical importance, in which the theory exhibits a failure surface. The plastic flow properties so established are compared with those of conventional plasticity theory; it is shown that the two theories, in general, exhibit substantially different plastic flow rules. Also, proofs are given which show that the new endochronic theory satisfies the Postulate of Isotropy and Drucker's Postulate of Stability in the Small.

1. INTRODUCTION

Endochronic plasticity was first introduced by Valanis[1, 2] in 1971 as an alternate approach for describing the inelastic behavior of history-dependent materials. The theory was founded upon the concepts of irreversible thermodynamics of internal variables, and formulated on the hypothesis that the current state of stress in a material is a functional of the entire history of deformation. The key to the theory is that the deformation history is defined, however, with respect to a deformation memory scale, called intrinsic time, which is itself a property of the material at hand. The resulting theory provides a unified approach for describing the elastic–plastic behavior of materials which do not require the notion of yield surface nor the specification of a loading function to distinguish loading from unloading. In essence, it predicts that plastic flow will occur from the onset of loading, a feature which is experimentally observed for numerous materials, including metals and granular materials.

In the early version of endochronic theory[1, 2], the intrinsic time was defined in terms of the strain tensor. This resulted in a theory having several features which were inconsistent with the observed behavior of most materials. In 1979, Valanis[3] developed a new version of endochronic plasticity theory which does not suffer from these shortcomings. In this new theory, the intrinsic time is defined in terms of the plastic strain tensor. Since its introduction, the new theory has been applied with remarkable success to various problems in metal plasticity[4, 5], soils[6] and concrete[7]. Despite this success, however, little has been done to establish the general plasticity properties of this new theory, particularly as they relate to the more conventional forms of elasto-plasticity. An understanding of these properties and their compatibility with measured material properties, is, of course, necessary for establishing the basic validity of the theory on physical grounds for various classes of materials.

An initial effort to explore the plastic properties of the new endochronic theory was undertaken by Trangenstein and Read[8], who considered the case of non-proportional deviatoric loading involving an abrupt change in loading direction. The results from their study, while somewhat limited by conditions to be discussed in the sequel, clearly showed that the plasticity features of the new endochronic theory, in general, differ greatly from those of classical plasticity. Nevertheless, some confusion has arisen lately in the literature regarding this issue[9, 10].

The purpose of the present paper is to further extend the study of the general properties of endochronic plasticity initiated by Trangenstein and Read[8] and, in particular, to consider the case in which a failure surface exists. Where possible, analytical methods are employed for this purpose and, in those cases where such methods prove to be intractable,

† Consultant; also, Associate Professor of Applied Mechanics, University of California, San Diego, U.S.A.

numerical methods are utilized to examine the theory. The plastic flow properties so established are compared with those from conventional plasticity; it is shown that the two theories exhibit, in general, substantially different flow rules. Finally, proofs are given in the Appendix which show that the new endochronic plasticity theory satisfies the Postulate of Isotropy and Drucker's Postulate of Stability in the Small.

2. BASIC EQUATIONS

We shall consider the deviatoric portion of the new endochronic theory, and attempt to establish some of its basic properties of plastic flow, especially for the case in which a failure surface exists. For small, isothermal deformation, and assuming plastic incompressibility, the basic equations of the new endochronic theory for deviatoric response are as follows:

$$\underline{s} = \int_0^z \rho(z-z') \frac{\mathrm{d}\underline{e}^p}{\mathrm{d}z'} \, \mathrm{d}z' \tag{1}$$

$$\mathrm{d}z = \frac{\mathrm{d}\zeta}{f(z)}, \tag{2}$$

where

$$\mathrm{d}\zeta = \|\mathrm{d}\underline{e}^p\| \tag{3}$$

$$\mathrm{d}\underline{e}^p = \mathrm{d}\underline{e} - \frac{\mathrm{d}\underline{s}}{2G} \tag{4}$$

and, by definition:

$$\mathrm{d}\underline{e} = \mathrm{d}\underline{\varepsilon} - \tfrac{1}{3} tr(\underline{\varepsilon}) \underline{I}. \tag{5}$$

Here, $\underline{s}$, $\underline{e}$ and $\underline{e}^p$ denote, respectively, the deviatoric stress, the deviatoric strain and the plastic deviatoric strain, while $\underline{\varepsilon}$ is the total strain. The variable z is termed the intrinsic time, while ζ describes the path length traversed by a deformation process in the 5-dimensional plastic deviatoric strain space, with suitable metric. In addition, $f(z)$ is a smooth positive function which provides for hardening, and G is the shear modulus. The double bars around a symbol denote its Euclidean norm.

The kernel function ρ is a weakly singular function of z, satisfying the condition $\rho(0) = \infty$ such that

$$\Phi(z) = \int_0^z \rho(y) \, \mathrm{d}y \tag{6}$$

exists for all $z \geqslant 0$. The weakly singular nature of $\rho(z)$ is a crucial feature of the theory for two reasons: (1) it provides for closure of hysteresis loops in the uniaxial or shear stress–strain space, however, small they may be, and (2) it ensures that, at points of unloading or reloading, the response is instantaneously elastic[3].

It will be assumed below that $\rho(z)$ is of the following general form:

$$\rho = g(z) z^{-\alpha} \tag{7}$$

where $0 < \alpha < 1$ and $g(z)$ is a positive, continuous function. Depending upon the particular forms of $g(z)$ and $f(z)$, the theory will or will not possess a failure surface. In the sequel, we set $f(z) = 1$ for convenience. Conditions on $g(z)$ which lead to a failure surface are addressed in the following section.

3. CONDITION FOR THE EXISTENCE OF A FAILURE SURFACE

To determine the conditions on the function $g(z)$ under which the theory described by eqns (1)–(5) possess a failure surface, consider the case of proportional loading in the deviatoric plane. Denoting by $\underset{\sim}{n}$ the unit tensor in the direction of loading, we can write

$$\underset{\sim}{s} = s\underset{\sim}{n}, \qquad \underset{\sim}{\varepsilon}^p = \underset{\sim}{n}\varepsilon^p, \qquad \mathrm{d}\underset{\sim}{\varepsilon}^p = \underset{\sim}{n}\,\mathrm{d}z, \qquad \|\underset{\sim}{n}\| = 1, \tag{8}$$

so that eqn (1) becomes:

$$s = \int_0^z \rho(z-z')\,\mathrm{d}z' = \int_0^z \rho(z')\,\mathrm{d}z'. \tag{9}$$

Since $\rho(z) > 0$ for all z, a failure surface will exist if the following condition is satisfied:

$$\lim_{z\to\infty} s = \lim_{z\to\infty} \int_0^z \rho(z')\,\mathrm{d}z' = \lim_{z\to\infty} \int_0^z \frac{g(y)}{y^\alpha}\,\mathrm{d}y \leqslant M, \tag{10}$$

where M is a positive constant. Since $g(y)$ is assumed to be a positive, continuous function, the above condition is satisfied when†

$$\lim_{z\to\infty} \int_0^z g(y)\,\mathrm{d}y \leqslant M_0, \tag{11}$$

where M_0 is a positive constant, subject to the condition that $g(y)y^{-\alpha}$ is weakly singular at $y = 0$.

A particular form of $g(z)$ which has been used widely and successfully in the literature in applications of the endochronic theory to various materials is

$$g(z) = \rho_0 e^{-\beta z}, \tag{12}$$

where ρ_0 and β are positive constants. From condition (11), it follows that for the above form of $g(z)$ a failure surface exists. This can also be shown by noting that with

$$\rho = \rho_0 \frac{e^{-\beta z}}{z^\alpha} \tag{13}$$

it follows from eqn (9) that

$$s = \rho_0 \int_0^z \frac{e^{-\beta y}}{y^\alpha}\,\mathrm{d}y = \rho_0 \beta^{-(1-\alpha)} \gamma(1-\alpha, \beta z) \tag{14}$$

where $\gamma(1-\alpha, \beta z)$ denotes the incomplete gamma function. Thus,

$$s_\infty = \lim_{z\to\infty} s = \rho_0 \beta^{-(1-\alpha)} \Gamma(1-\alpha), \tag{15}$$

where $\Gamma(1-\alpha)$ is the gamma function, thereby showing that s limits to a finite number as z tends to infinity. Since the direction $\underset{\sim}{n}$ of loading is arbitrary, eqn (15) shows that, when $f(z) = 1$, the failure surface for radial loading is a circle in the deviatoric plane.

For an arbitrary stress path, eqn (1) with $f(z) = 1$ yields

$$|s_{ij}| \leqslant \int_0^z \rho(y)\,\mathrm{d}y. \tag{16}$$

† For proof, see Ref. [11], p. 653.

Inequality (16) implies that each stress component is bounded by eqn (15). This together with the result for radial loading indicates that for arbitrary stress paths the failure surface is bounded by the circle in the π-plane defined by eqn (15).

In the remainder of this paper, the form of $\rho(z)$ given by eqn (13) will be adopted for the purpose of exploring the plastic flow properties of the version of the theory which exhibits a failure surface.

4. LIMITING CASES OF RESPONSE TO SMOOTH STRAIN PATHS

In this section, two limiting cases of the model's response to smooth strain paths are considered, namely (a) response for small z near the origin of the deviatoric plane and (b) response for large values of z as a failure surface is approached. A knowledge of the model's response to these two cases provides a further understanding of its characteristics and is useful in assessing the numerical results presented in Section 6.

4.1. *Response for small z near the origin of deviatoric space*

Consider eqn (1), which may be differentiated to give:

$$\frac{\mathrm{d}\underline{\xi}}{\mathrm{d}z} = \rho(z)\underline{a}(0) + \int_0^z \rho(y)\underline{a}'(z-y)\,\mathrm{d}y \tag{17}$$

in which

$$\underline{a} \equiv \frac{\mathrm{d}\underline{\varepsilon}^p}{\mathrm{d}z}, \qquad \underline{a}' \equiv \frac{\mathrm{d}}{\mathrm{d}z}\underline{a} \tag{18}$$

where $\underline{a}$ is a unit tensor. For smooth strain paths, we can write:

$$\begin{aligned} \underline{a}(0) &= \underline{a}(z) + \sum_{n=1}^{\infty} \frac{1}{n!}(-z)^n \underline{a}^n(z) \\ \underline{a}'(z-y) &= \sum_{n=0}^{\infty} \frac{(-1)^n}{n!} y^n \underline{a}^{n+1}(z). \end{aligned} \tag{19}$$

Substituting eqn (19) into eqn (17) leads to the expression

$$\frac{\mathrm{d}\underline{\xi}}{\mathrm{d}z} = \rho(z)\underline{a}(z) + \sum_{n=1}^{\infty} \frac{1}{n!}(-z)^n \rho(z)\underline{a}^n(z) + \underline{a}'(z)\int_0^z \rho(y)\,\mathrm{d}y + \sum_{n=1}^{\infty} \frac{(-1)^n}{n!}\underline{a}^{n+1}(z)\int_0^z y^n \rho(y)\,\mathrm{d}y. \tag{20}$$

Since $\rho(z) \sim z^{-\alpha}$, it follows that:

$$\begin{aligned} z^n \rho(z) &= 0(z^{n-\alpha}) \\ \int_0^z \rho(y)\,\mathrm{d}y &= 0(z^{1-\alpha}) \\ \int_0^z y^n \rho(y)\,\mathrm{d}y &= 0(z^{n+1-\alpha}). \end{aligned} \tag{21}$$

Consequently, eqn (20) can be expressed as:

$$\frac{\mathrm{d}\underline{\xi}}{\mathrm{d}z} \doteq \rho(z)\underline{a}(z) + 0(z^{1-\alpha}), \tag{22}$$

from which it follows that, for $z \ll 1$, the tangent to the stress path $\underline{\xi}$ and $\underline{a}$ are coaxial, since $0 < \alpha < 1$. Therefore, $\mathrm{d}\underline{\xi}$ and $\mathrm{d}\underline{\varepsilon}^p$ are also coaxial.

4.2. *Response for large z near a failure surface*

Consider eqn (1) with $\rho(z)$ defined according to eqn (13). By making a change of variable, we can write:

$$\underline{\xi} = \rho_0 \int_0^z \frac{e^{-\beta y}}{y^\alpha} \underline{\varepsilon}(z-y)\, dy. \tag{23}$$

To explore the asymptotic behavior of this equation as the failure surface is approached, we consider smooth plastic strain paths and investigate the limiting form of eqn (23) as $z \to \infty$. For a wide class of materials, including metals, concrete and rock, it transpires that $\beta \gg 1$ (actually of order 10^4). When this is the case, the integral in eqn (23) can be evaluated asymptotically for large βz by using Watson's lemma.† Following this approach, it is noted that for large βz, the major contribution to the above integral occurs near $y = 0$. Because of the assumed smoothness of the $\underline{\varepsilon}^p$-path, the function $\underline{\varepsilon}(z-y)$ can be expanded in a Taylor series about $y = 0$, i.e.

$$\underline{\varepsilon}(z-y) = \underline{\varepsilon}(z) - y\underline{\varepsilon}'(z) + \frac{y^2}{2}\underline{\varepsilon}''(z) - \cdots \tag{24}$$

Consider now a stress path which is arbitrary for $z < z_0$ but, at z_0, monotonically approaches the failure surface. For $z > z_0$, $\underline{\varepsilon}$ will be smooth and simple during its recent past $\{z-y \mid 0 \leqslant y \leqslant y_m\}$, where y_m is a characteristic of the material such that for $y \geqslant y_m$, $e^{-\beta y}$ is negligible. For such paths, $\underline{\varepsilon}$ can be represented by the first few terms of the series expansion (24) over $\{0 \leqslant y \leqslant y_m\}$ where $e^{-\beta y}$ takes on significant values.

Hence, eqn (23) can be expressed as:

$$\underline{\xi} = \rho_0 \int_0^\infty \frac{e^{-\beta y}}{y^\alpha} [\underline{\varepsilon}(z) - y\underline{\varepsilon}'(z) + \cdots]\, dy + 0(e^{-\beta z}). \tag{25}$$

Applying Watson's lemma to the first integral on the r.h.s. of eqn (25), we obtain the result

$$\underline{\xi} = \rho_0 \left[\underline{\varepsilon}(z) \frac{\Gamma(1-\alpha)}{\beta^{1-\alpha}} - \underline{\varepsilon}'(z) \frac{\Gamma(2-\alpha)}{\beta^{2-\alpha}} + 0\left(\frac{1}{\beta^{3-\alpha}}\right) \right] + 0(e^{-\beta z}) \tag{26}$$

as $\beta z \to \infty$. This expression may be rewritten, using eqn (16) and the relation $\Gamma(n+1) = n\Gamma(n)$, in the form:

$$\underline{\xi} = s_\infty \left[\underline{\varepsilon} - c\underline{\varepsilon}' + \frac{1}{2}c^2 \left(\frac{2-\alpha}{1-\alpha}\right) \underline{\varepsilon}'' - \frac{1}{6}c^3 \left(\frac{2-\alpha}{1-\alpha}\right)\left(\frac{3-\alpha}{1-\alpha}\right) \underline{\varepsilon}''' + \cdots \right], \tag{27}$$

where we have set

$$c = \frac{1-\alpha}{\beta}. \tag{28}$$

Taking the norm of both sides leads to the expression

$$\|\underline{\xi}\| = s_\infty \left[1 - c^2 \left\{ 1 + \frac{1}{2}\left(\frac{2-\alpha}{1-\alpha}\right) \right\} (\underline{\varepsilon}' \cdot \underline{\varepsilon}') + 0(\beta^{-3}) \ldots \right]^{1/2} \tag{29}$$

where use has been made of the fact that $\underline{\varepsilon} \cdot \underline{\varepsilon} = 1$ and $\underline{\varepsilon} \cdot \underline{\varepsilon}' = 0$. It then follows from eqn

† See, for instance, Ref. [12].

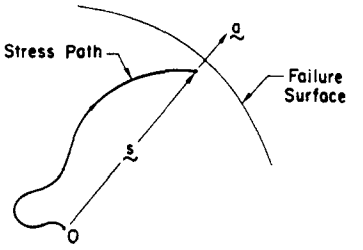

Fig. 1. Stress path in the π-plane, showing $\underset{\sim}{q}$ becoming coaxial with $\underset{\sim}{s}$ as failure surface is approached.

(29) that as $\underset{\sim}{s}$ approaches the failure surface, $\|\underset{\sim}{s}\| \to s_\infty$, which can occur only if $q' \to 0$. Therefore, it follows from eqn (27) that as the failure surface is approached, $\underset{\sim}{s}$ becomes coaxial with $\underset{\sim}{q}$, and hence with $\mathrm{d}\underset{\sim}{\varepsilon}^p$. Consequently, if the trace of the failure surface in the deviatoric plane is a circle, $\mathrm{d}\underset{\sim}{\varepsilon}^p$ will become normal to this surface as $\underset{\sim}{s}$ approaches the surface, as depicted in Fig. 1. This feature of the theory will be illustrated via examples in the numerical studies presented in Section 6.

5. RESPONSE TO AN ABRUPT CHANGE IN LOADING DIRECTION

Important insight into the constitutive properties of complex constitutive theories can often be obtained by examining their response to an abrupt change in loading direction from an otherwise smooth stress path. This approach was adopted by Trangenstein and Read[8] to explore the inelastic properties of the new endochronic theory and it is also followed here. We begin with a review of the analysis by Trangenstein and Read[8], and show that the form of the asymptotic expansion which was assumed in their analysis, is of limited validity and applies only to a small class of stress paths. A more general form of asymptotic expansion is then introduced into the analysis, which leads to results which appear to have general validity.

5.1. *Previous study*

Trangenstein and Read[8] recently considered the response of the new endochronic model to an abrupt, arbitrary change in loading direction from a previously smooth stress path. These authors focused on the same form of endochronic model that is considered in the present paper, with the kernel function having the general form given by eqn (7). Using asymptotic expansions, the characteristics of the model were determined for infinitesimal loading increments, $\mathrm{d}\underset{\sim}{s}$, in a new arbitrary direction $\underset{\sim}{b}$ in stress space from a previously smooth stress path, as shown in Fig. 2. The tangent to the smooth stress path at the point of abrupt change in stress direction will be denoted by $\underset{\sim}{t}$, where both $\underset{\sim}{b}$ and $\underset{\sim}{t}$ are unit vectors. The analysis of Ref. [8] then showed that (a) the preceding plastic strain increment, $\mathrm{d}\underset{\sim}{\varepsilon}^p$, is coaxial with $\underset{\sim}{t}$, and (b) the incremental inelastic compliance, C^p, varies with the direction $\underset{\sim}{b}$

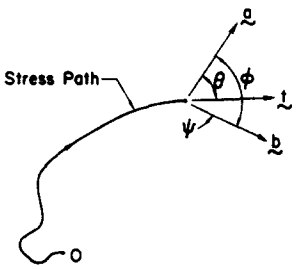

Fig. 2. Smooth stress path in the π-plane, showing the unit vectors $\underset{\sim}{q}$, $\underset{\sim}{b}$ and $\underset{\sim}{t}$ and the angles θ, ϕ and ψ.

of the new stress increment according to the expression:

$$C_p \equiv \left\| \frac{d\underline{\varepsilon}^p}{d\underline{\sigma}} \right\| = \begin{cases} \dfrac{\cos\psi}{\gamma_0}, & \psi < \dfrac{\pi}{2} \\ 0, & \psi \geqslant \dfrac{\pi}{2} \end{cases} \tag{30}$$

when there is no hardening in the model, i.e. $f(z) = 1$. In eqn (30), γ_0 is defined as

$$\gamma_0 = \alpha_1 g(0)\Gamma(1-\alpha)\Gamma(1+\alpha)/\Gamma(2) \tag{31}$$

where α_1 is a positive constant and $\Gamma(\ )$ denotes the gamma function. Furthermore, ψ is the angle between the vectors $\underline{h}$ and $\underline{t}$, so that we can write

$$\cos\psi = \underline{h}\cdot\underline{t}. \tag{32}$$

Equation (30) indicates that whenever the new loading direction $\underline{h}$ makes an angle ψ of less than $\pi/2$ with the tangent to the stress path $\underline{t}$, the response of the model will be inelastic. On the other hand, whenever ψ is equal to or greater than $\pi/2$, the response will be purely elastic, but only in the infinitesimal neighborhood of the abrupt change in loading direction. These response characteristics obviously differ substantially from those of classical plasticity, as noted in Refs [8, 10].

It is important to note that the analysis of Trangenstein and Read[8] was based upon an assumed form of asymptotic expansion which actually forces the plastic strain increment $d\underline{\varepsilon}^p$, to be coaxial with $\underline{t}$ for a smooth stress path; this constraint is not generally valid, especially for stress states near a failure surface as shown in Section 4.2. Such a constraint can be eliminated by adopting a more general form of asymptotic expansion in the analysis, which is done below.

In that which follows, the response of the endochronic model to an abrupt change in loading direction in stress space is reanalyzed using a more general form of asymptotic expansion than adopted in Ref. [8]. It is shown that the resulting response characteristics differ considerably from those found in Ref. [8] and are in agreement with corresponding numerical studies and limiting cases considered herein.

5.2. *New analysis*

Consider a deviatoric stress path that is smooth for $0 \leqslant z \leqslant z_0^-$ and, at $z = z_0$, suddenly changes direction so that, for $z \geqslant z_0^+$, the deviatoric stress increment, $d\underline{\sigma}$, lies in a new direction $\underline{h}$.† For $z_0^+ \leqslant z \leqslant z_0 + \Delta z$, we consider an asymptotic expansion for $\underline{\sigma}$ of the form:

$$\underline{\sigma}(z_0+\Delta z) \doteq \underline{\sigma}(z_0) + \underline{h}k\Delta z^q, \tag{33}$$

where $q > 0$ and k are to be determined. Furthermore, upon setting

$$\Delta\underline{\sigma}(z_0) \equiv \underline{\sigma}(z_0+\Delta z) - \underline{\sigma}(z_0), \tag{34}$$

we can use eqns (1) and (13) to write

$$\Delta\underline{\sigma}(z_0) \doteq \Delta z\underline{t}\left\|\frac{d\underline{\sigma}}{dz}\right\|_{z_0^-} + \int_0^{\Delta z} \rho_0 \frac{e^{-\beta y}}{y^\alpha}[\underline{\varrho}(z_0+\Delta z-y) - \underline{\varrho}(z_0-y)]\,dy \tag{35}$$

† Here, z_0^- and z_0^+ are the left and right neighborhood values of z_0, respectively.

where

$$\underline{\ell}\left\|\frac{d\underline{\varrho}}{dz}\right\|_{z_0^-}=\left.\frac{d\underline{\varrho}}{dz}\right|_{z_0^-}\equiv\rho_0\frac{e^{-\beta z_0}}{z_0^\alpha}\underline{q}(0)+\int_0^{z_0^-}\rho_0\frac{e^{-\beta y}}{y^\alpha}\underline{q}'(z_0-y)\,dy. \tag{36}$$

Consider now the asymptotic expansion for $\underline{q}(z_0+\Delta z)$. This expansion should be expressed in terms of two linearly independent vectors, one of which must be $\underline{b}$. For the other vector, we have $\underline{q}$ and $\underline{\ell}$ available, since they are both linearly independent of $\underline{b}$. If $\underline{q}$ is selected for this purpose, as was done in Ref. [8], it restricts $\underline{q}$ to be coaxial with $\underline{\ell}$, a condition which is not correct for stress states near a failure surface (see Section 4.2). Therefore, it appears that the appropriate vectors to use in the asymptotic expansion for $\underline{q}(z_0+\Delta z)$ are $\underline{b}$ and $\underline{\ell}$ and, on this basis, we adopt the following form for the asymptotic expansion of $\underline{q}$:

$$\underline{q}(z_0+\Delta z)-\underline{q}(z_0)\doteq-\underline{\ell}\alpha_1\Delta z^u+\underline{b}(\beta_0+\beta_1\Delta z^p) \tag{37}$$

where α_1, β_0, β_1, u and p are constants. We shall also assume that

$$\beta_0+\beta_1\Delta z^p>0 \qquad \text{for} \qquad \Delta z>0. \tag{38}$$

Upon substituting eqn (37) into eqn (35), and using the expansions for the integrals involving $\rho(z)$ given in Ref. [8], it follows that

$$\Delta\underline{\varrho}(z_0)\doteq\underline{\ell}\left\{\Delta z\left\|\frac{d\underline{\varrho}}{dz}\right\|_{z_0^-}-\alpha_1\rho_0\frac{\Gamma(1-\alpha)\Gamma(1+u)}{\Gamma(2+u-\alpha)}\Delta z^{1+u-\alpha}\right\}$$
$$+\underline{b}\left\{\frac{\rho_0\beta_0}{1-\alpha}\Delta z^{1-\alpha}+\rho_0\beta_1\frac{\Gamma(1-\alpha)\Gamma(1+p)}{\Gamma(2+p-\alpha)}\Delta z^{1+p-\alpha}\right\}. \tag{39}$$

However, the new stress increment, $\Delta\underline{\varrho}$, at the point of the abrupt change in loading direction was prescribed in the arbitrary direction $\underline{b}$, in eqn (33). As a result, the coefficient of $\underline{\ell}$ in eqn (39) must vanish, which leads to the following conditions:

$$\begin{aligned}u&=\alpha\\ \alpha_1&=\left\|\frac{d\underline{\varrho}}{dz}\right\|_{z_0^-}\Gamma(2)/\{\rho_0\Gamma(1-\alpha)\Gamma(1+\alpha)\}.\end{aligned} \tag{40}$$

Let†

$$\begin{aligned}\cos\theta&\equiv\underline{q}\cdot\underline{\ell}\\ \cos\phi&\equiv\underline{q}\cdot\underline{b}\end{aligned} \tag{41}$$

and note that for the unit vector $\underline{q}$:

$$\|\underline{q}(z_0+\Delta z)\|^2=1. \tag{42}$$

Upon substituting eqns (37), (40) and (41) into eqn (42), it follows that:

$$1\doteq\{1+\beta_0(\beta_0+2\cos\phi)\}-2\alpha_1(\cos\theta+\beta_0\cos\psi)\Delta z^\alpha$$
$$+2\beta_1(\cos\phi+\beta_0)\Delta z^p+\beta_1^2\Delta z^{2p}+\alpha_1^2\Delta z^{2\alpha}-2\alpha_1\beta_1\cos\psi\Delta z^{\alpha+p}. \tag{43}$$

(i) Consider the case $\cos\phi>0$. The zero order terms in eqn (43), together with the non-

† It can be shown (see Appendix) that $\cos\theta>0$.

negative condition from eqn (38), require that

$$\beta_0 = 0. \tag{44}$$

The next higher order terms in eqn (43), together with eqn (40a) imply that

$$p = u = \alpha \tag{45}$$

$$\beta_1 = \alpha_1 \cos\theta/\cos\phi. \tag{46}$$

Upon substituting eqns (44)–(46) into eqn (39), we find

$$\left.\frac{d\underline{\varepsilon}}{dz}\right|_{z_0^+} \equiv \lim_{\Delta z \to 0} \frac{\Delta \underline{\varepsilon}}{\Delta z} = \underline{b}\frac{\cos\theta}{\cos\phi}\left\|\frac{d\underline{\varepsilon}}{dz}\right\|_{z_0^-}. \tag{47}$$

The finite value of $d\underline{\varepsilon}/dz$ at z_0^+ implies plastic response for this case.

(ii) Consider the case $\cos\phi = 0$. In this instance, the zero order terms must satisfy eqn (44), while the next higher order terms require that

$$-2\alpha_1 \cos\theta \Delta z^{\alpha} + \beta_1^2 \Delta z^{2p} = 0. \tag{48}$$

Thus,

$$p = \frac{u}{2} = \frac{\alpha}{2} \tag{49}$$

$$\beta_1 = (2\alpha_1 \cos\theta)^{1/2}. \tag{50}$$

Upon substituting eqns (49) and (50) into eqn (39), we find that

$$\left.\frac{d\underline{\varepsilon}}{dz}\right|_{z_0^+} \to \infty, \tag{51}$$

implying that the response is purely elastic.

(iii) Finally, consider the case $\cos\phi < 0$. The zero order terms in eqn (43) must satisfy the condition

$$\beta_0 = -2\cos\phi \tag{52}$$

while the next higher order terms require that

$$p = \alpha. \tag{53}$$

Inasmuch as $\beta_0 \neq 0$, we obtain in this case the condition (51), implying that the response is purely elastic.

The results of the above analysis can be conveniently expressed in terms of the incremental plastic compliance, C^p, as follows:

$$C^p \equiv \left\|\frac{d\underline{\varepsilon}^p}{d\underline{\varepsilon}}\right\| = \begin{cases} \dfrac{\cos\phi}{F(z_0)}, & \phi < \dfrac{\pi}{2} \\ 0, & \phi \geqslant \dfrac{\pi}{2} \end{cases} \tag{54}$$

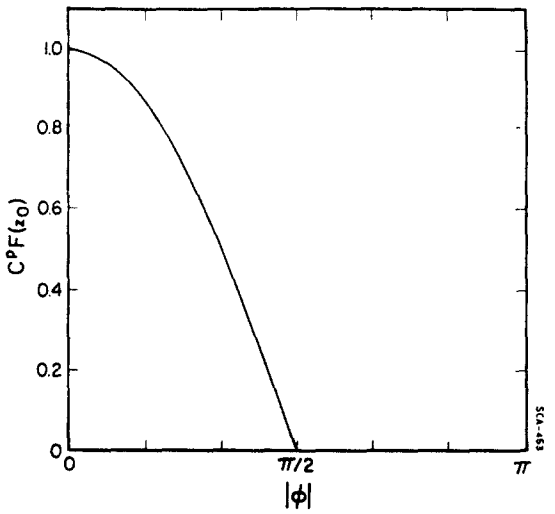

Fig. 3. Variation of incremental plastic compliance with angle ϕ.

where

$$F(z_0) \equiv \cos\theta \left\| \frac{d\underset{\sim}{\xi}}{dz} \right\|_{z_0^-}. \tag{55}$$

Equation (54) reveals that C^p is a continuous function of the angle ϕ and is zero for all stress increments normal to $\underset{\sim}{q}$, as well as for those which have a negative component with respect to $\underset{\sim}{q}$ at z_0^-, as depicted in Fig. 3. In addition, C^p depends upon $\|d\underset{\sim}{\xi}/dz\|_{z_0}$, which approaches zero as a failure surface is approached. Note also that C^p depends upon the angle θ between the unit vectors $\underset{\sim}{q}$ and $\underset{\sim}{t}$ and that this angle depends upon the plastic strain history. Except for proportional loading, in which case $\underset{\sim}{q}$ and $\underset{\sim}{t}$ are coaxial, numerical methods must be utilized to explore the properties of the plastic compliance, C^p; this is done in Section 6 for a number of smooth complex stress paths.

For the special case of proportional loading, $\underset{\sim}{q}$ and $\underset{\sim}{t}$ are coaxial so that $\psi = \phi$. In this case, it is straightforward to show that eqn (54) reduces to the expression for C^p given in Ref. [8].

6. NUMERICAL STUDY OF COMPLEX STRESS AND STRAIN PATHS

The response of the new endochronic model to various prescribed complex (non-proportional) stress and strain paths is investigated in this section using numerical procedures. An incremental numerical approach developed for this purpose is described, and the results obtained from applying it to study the response of the model to a number of complex paths are presented; these results aid in defining the inelastic characteristics of the model for stress states that lie between the two limiting cases treated in Section 4.

6.1. *Numerical scheme*

Valanis and Read[6] have shown that the weakly singular kernel function, $\rho(z)$, of the new endochronic theory can be expressed in terms of a Dirichlet series:

$$\rho(z) = \sum_{r=1}^{\infty} R_r e^{-\alpha_r z} \tag{56}$$

where, in order to satisfy the Clausius–Duhem inequality, it is necessary that $\alpha_r \geqslant 0$ and $R_r \geqslant 0$ for all r. Moreover, to ensure that $\rho(z)$ is singular at the origin and integrable over

a finite domain of z, we must have

$$\sum_{r=1}^{\infty} R_r = \infty, \qquad \sum_{r=1}^{\infty} \frac{R_r}{\alpha_r} < \infty. \tag{57a, b}$$

In past applications of the theory, it has been found that two or three terms of the series (56) are usually quite adequate for representing $\rho(z)$; in such cases, however, care must be taken to ensure that the infinitely large value of $\rho(0)$ is approximated by a suitably large finite value. When this is done, we can write

$$\rho(z) \doteq \sum_{r=1}^{n} R_r e^{-\alpha_r z} \tag{58}$$

when n is finite. Substitution of eqn (58) into eqn (1) yields the following expression for $\underset{\sim}{\xi}$:

$$\underset{\sim}{\xi} = \sum_{r=1}^{n} \underset{\sim}{Q}_r, \tag{59}$$

where

$$\underset{\sim}{Q}_r = R_r \int_0^z e^{-\alpha_r (z-z')} \frac{\mathrm{d}\underset{\sim}{\varepsilon}^p}{\mathrm{d}z'} \, \mathrm{d}z'. \tag{60}$$

Differentiation of this equation gives the following linear first order differential equation:

$$\frac{\mathrm{d}\underset{\sim}{Q}_r}{\mathrm{d}z} + \alpha_r \underset{\sim}{Q}_r = R_r \frac{\mathrm{d}\underset{\sim}{\varepsilon}^p}{\mathrm{d}z}, \tag{61}$$

which, together with eqn (59), allows one to write

$$\mathrm{d}\underset{\sim}{\xi} = R \, \mathrm{d}\underset{\sim}{\varepsilon}^p - \underset{\sim}{Q} \, \mathrm{d}z, \tag{62}$$

where

$$R = \sum_{r=1}^{n} R_r, \qquad \underset{\sim}{Q} = \sum_{r=1}^{n} \alpha_r \underset{\sim}{Q}_r. \tag{63a, b}$$

Equations (61)–(63) provide a simple approach for incrementally integrating the stress, $\underset{\sim}{\xi}$, which is considerably more attractive from a computational standpoint than numerically coping with the hereditary integral in eqn (1).

In that which follows, explicit numerical schemes are presented for incrementally updating the governing equations of the new endochronic theory when either the strain or stress histories are given. Because of the explicit nature of the schemes, it is necessary that the increments be taken sufficiently small to ensure accuracy.

Prescribed strain history. It is assumed that $\underset{\sim}{\xi}$, $\underset{\sim}{\varepsilon}$, $\underset{\sim}{\varepsilon}^p$, $\underset{\sim}{Q}_r$, and $\underset{\sim}{Q}$ are known at the beginning of each known increment of strain, $\Delta\underset{\sim}{\varepsilon}$. Using eqn (62), we can write

$$\Delta\underset{\sim}{\xi} = \sum_{r=1}^{n} \Delta\underset{\sim}{Q}_r = R\,\Delta\underset{\sim}{\varepsilon}^p - \underset{\sim}{Q}\,\Delta z, \tag{64}$$

while the incremental Hooke's law, eqn (4), yields

$$\Delta\underset{\sim}{\xi} = 2G(\Delta\underset{\sim}{\varepsilon} - \Delta\underset{\sim}{\varepsilon}^p). \tag{65}$$

Substitution of eqn (65) into eqn (64) leads to the expression

$$\Delta \underset{\sim}{\varepsilon} + \frac{1}{2G} \underset{\sim}{Q} \Delta z = \left(1 + \frac{R}{2G}\right) \Delta \underset{\sim}{\varepsilon}^p. \tag{66}$$

Upon taking the inner product of eqn (66) with itself, and using eqns (2) and (3) with $f(z) = 1$, it follows that

$$\left\{\left(\frac{1}{2G}\right)^2 \underset{\sim}{Q} \cdot \underset{\sim}{Q} - \left(1 + \frac{R}{2G}\right)^2\right\} \Delta z^2 + \frac{1}{G} \underset{\sim}{Q} \cdot \Delta \underset{\sim}{\varepsilon} \Delta z + \Delta \underset{\sim}{\varepsilon} \cdot \Delta \underset{\sim}{\varepsilon} = 0. \tag{67}$$

For given $\Delta \underset{\sim}{\varepsilon}$ and $\underset{\sim}{Q}$, eqn (67) provides a quadratic equation for the unknown Δz. Once Δz is known, $\Delta \underset{\sim}{\varepsilon}^p$ can be obtained from eqn (66) and $\Delta \underset{\sim}{\sigma}$ can then be determined by eqn (65). Equation (61) is used next to evaluate $\Delta \underset{\sim}{Q}_r$. This explicit integration scheme was originally developed by Valanis[13].

Prescribed stress history. For this case, $\underset{\sim}{\sigma}$, $\underset{\sim}{\varepsilon}$, $\underset{\sim}{\varepsilon}^p$, $\underset{\sim}{Q}_r$ and $\underset{\sim}{Q}$ are assumed to be known at the beginning of each known increment of stress, $\Delta \underset{\sim}{\sigma}$. Using eqn (62), we can write

$$R \Delta \underset{\sim}{\varepsilon}^p = \Delta \underset{\sim}{\sigma} + \underset{\sim}{Q} \Delta z. \tag{68}$$

Upon taking the inner product of eqn (68) with itself, and using eqns (2) and (3) with $f(z) = 1$, it follows that

$$(\underset{\sim}{Q} \cdot \underset{\sim}{Q} - R^2) \Delta z^2 + 2(\Delta \underset{\sim}{\sigma} \cdot \underset{\sim}{Q}) \Delta z + \Delta \underset{\sim}{\sigma} \cdot \Delta \underset{\sim}{\sigma} = 0, \tag{69}$$

which again is a quadratic equation for Δz. After solving for Δz, $\Delta \underset{\sim}{\varepsilon}^p$, $\Delta \underset{\sim}{Q}_r$ and $\Delta \underset{\sim}{\varepsilon}$ can be determined from eqns (68), (61) and (65), respectively.

6.2. *Numerical investigation of complex paths*

Using computer programs based upon the numerical schemes described above, the response of the new endochronic model is explored numerically in this section for a number of complex (non-proportional) stress and strain paths. For this purpose, a model was fit to copper data, which used three terms in the series (58), having the following values for α_r and R_r:

$$\begin{aligned} (\alpha_1, \alpha_2, \alpha_3) &= (0.767, 1.15, 2.75) \times 10^4 \\ (R_1, R_2, R_3) &= (0.46, 2.2, 5.9) \times 10^2 \text{ GPa}. \end{aligned} \tag{70}$$

Moreover, we set

$$G = 38.61 \text{ GPa}. \tag{71}$$

Consider, first, a prescribed strain path, having the triangular form shown in Fig. 4. The path starts at $\underset{\sim}{\varepsilon} = \underset{\sim}{0}$, proceeds along the ε_3-axis and continues in a counterclockwise direction. At various intervals along the path, the corresponding stress vectors predicted by the model are shown. Note that, after a sudden change in the direction of strain, the stress vector changes smoothly, gradually approaching coaxiality with the strain increment. Such behavior reflects the effect of fading memory inherent in the model, and has been experimentally observed by Ohashi *et al.*[14, 15] for metals. The response of a classical plasticity model with hardening to this strain path was also investigated and found to result in a similar variation of the stress vectors along the path.

Substantial differences between the new endochronic model and classical plasticity become apparent, however, by investigating prescribed stress paths. Consider, for example,

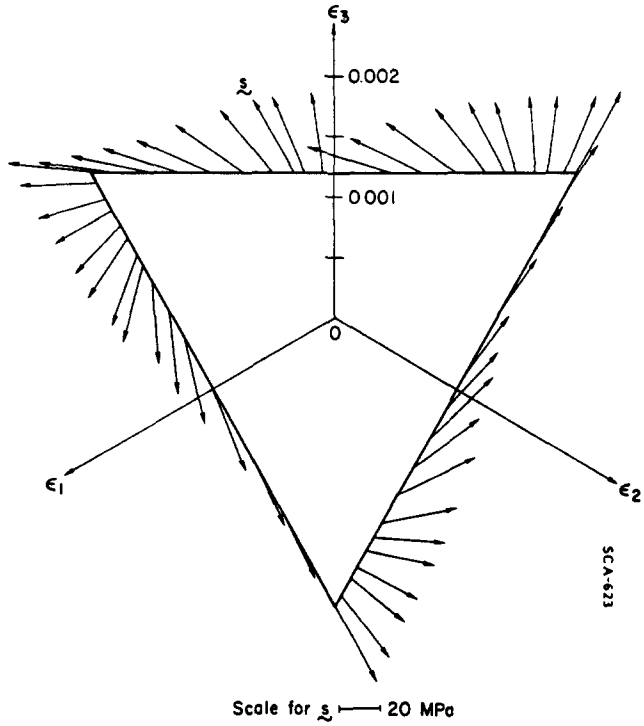

Fig. 4. Triangular strain path and corresponding stress vectors predicted by model.

the circular stress paths depicted in Fig. 5, where σ_y denotes the yield stress in simple tension. Here, the corresponding plastic strain increment vectors, $\Delta\underset{\sim}{\varepsilon}^p$, predicted by the new endochronic model at various points along the paths for the specified increments $\|\Delta\underset{\sim}{s}/\sigma_y\|$ are shown. Note that, in the cases of the two small circular paths shown in Fig. 5(a), the vectors, $\Delta\underset{\sim}{\varepsilon}^p$ are almost tangent to the stress paths for small z, which is consistent with results derived earlier in Section 4.1, and the radial component of $\Delta\underset{\sim}{\varepsilon}^p$ increases as the failure surface is approached, consistent with Section 4.2. As the failure surface is approached, $\Delta\underset{\sim}{\varepsilon}^p \to \infty$.

Next, consider the complex stress path shown in Fig. 6, which has a circular segment that is near to, and concentric with, a failure surface. The stress path starts at the origin, proceeds upward along the s_3-axis and then follows the circular segment in a clockwise fashion. The plastic strain increment vectors, $\Delta\underset{\sim}{\varepsilon}^p$, predicted by the model at various positions along the circular segment are shown in the figure. Note that these vectors are nearly perpendicular to the stress path and nearly coaxial with the stress, $\underset{\sim}{s}$. These features of the model are in full agreement with the analysis presented in Section 4.2 for the case of limiting behavior near a failure surface.

Figure 7 shows stress paths consisting of two linear segments. The paths start at the origin, proceed along the s_3-axis and then turn to follow linear paths, which make angles of 30°, 60° and 90° with the s_3-axis. Again, the plastic strain increment vectors, $\Delta\underset{\sim}{\varepsilon}^p$, predicted by the model at various locations along the second segment of each path are shown in the figures. For the paths depicted in Fig. 7(a), in which the second segment of the stress paths begins at $s_3 = \sigma_y/6$, the vector, $\Delta\underset{\sim}{\varepsilon}^p$, is initially almost tangent to the stress path, but becomes increasingly perpendicular to the failure surface as the failure surface is approached. For the paths shown in Fig. 7(b), the second segments begin at $s_3 = \sigma_y/3$, which is substantially closer to the failure surface than the point at which the second segments in Fig. 7(a) were initiated. As a result, the incremental vectors, $\Delta\underset{\sim}{\varepsilon}^p$, are not tangent to the stress path as before, but have a significant radial component which becomes increasingly dominant as the failure surface is approached. All of the above behavior is again fully consistent with the results derived in Section 4.

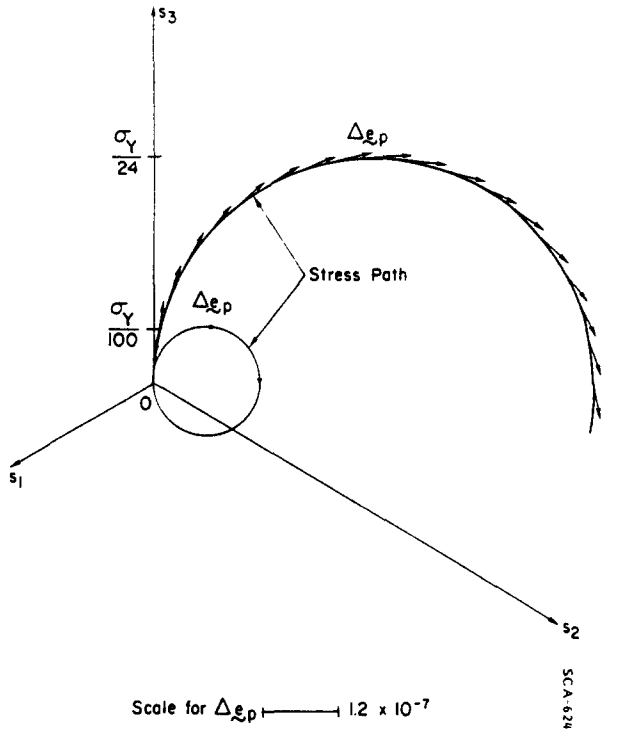

(a) Scale for $\Delta\underset{\sim}{\varepsilon}_p$ ⟼ 1.2×10^{-7}

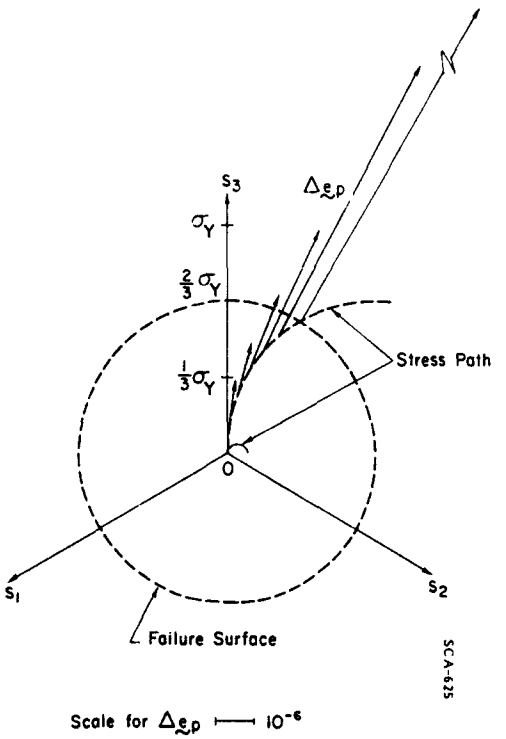

(b) Scale for $\Delta\underset{\sim}{\varepsilon}_p$ ⟼ 10^{-6}

Fig. 5. Circular stress paths and corresponding plastic strain increment vectors predicted by the model: (a) small radii paths near the origin, (b) large radius path.

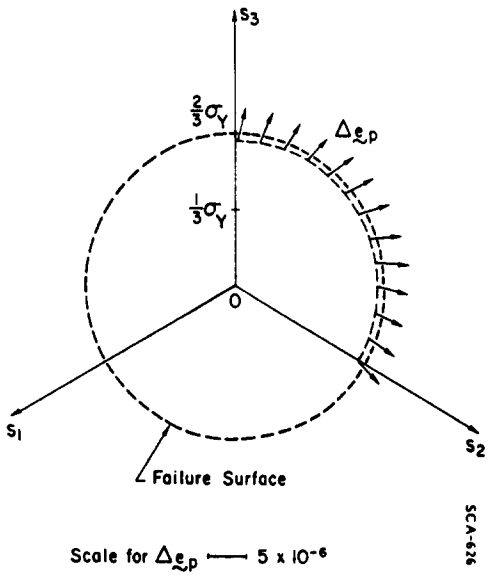

Fig. 6. Circular stress path near the failure surface and the corresponding plastic strain increment vectors predicted by the model.

Finally, consider the stress path shown in Fig. 8, which consists, first, of loading along the s_3-axis, followed by a triangular path traversed in a counterclockwise direction. The vectors, $\Delta\varepsilon^p$, predicted by the model at various positions along the triangular portion of the stress path are shown in the figure. Note that, after an abrupt change in the loading direction, the vector, $\Delta\varepsilon^p$, greatly diminishes in magnitude, reflecting the unloading that is occurring. An interesting and unique feature of the model is that no unloading or reloading criteria are required. Also, as the stress path approaches the failure surface, the vector, $\Delta\varepsilon^p$, becomes normal to this surface, again in agreement with the results from Section 4.

7. CONCLUSIONS

The purpose of this study was to explore the plastic flow and failure characteristics of the version of the new endochronic theory which exhibits a failure surface. Where possible, the inelastic characteristics of the model have been investigated theoretically and, in other cases, numerical methods have been developed and applied to establish various constitutive features of the model. The major results and conclusions from this study are summarized as follows:

1. The mathematical requirements which the kernel function $\rho(z)$ must satisfy so that the model will possess a failure surface were established. When these requirements are satisfied, and the hardening function $f(z)$ is set to unity, the model exhibits a failure surface whose trace in the π-plane is a circle.

2. The plastic flow properties of the endochronic model which exhibits a failure surface were theoretically established for two limiting cases, namely, (a) the response for small z near the origin and (b) the response for large z as failure is approached.

3. The previous analysis by Trangenstein and Read[8], concerning the response of the new endochronic model to an abrupt change in loading direction from an otherwise smooth stress path, was reviewed and found to have limited application, due to the specialized form of asymptotic expansion assumed. A more general asymptotic expansion was developed and used to reexamine the properties of the model under an abrupt change of loading direction. The results from this new analysis include those of Ref. [8] as a special case and, on the basis of other evidence presented herein, appear to have general validity.

4. The new analysis shows that, whenever a new loading direction makes an angle of less than $\pi/2$ with the preceding plastic strain increment, $d\varepsilon^p$, the new model will exhibit

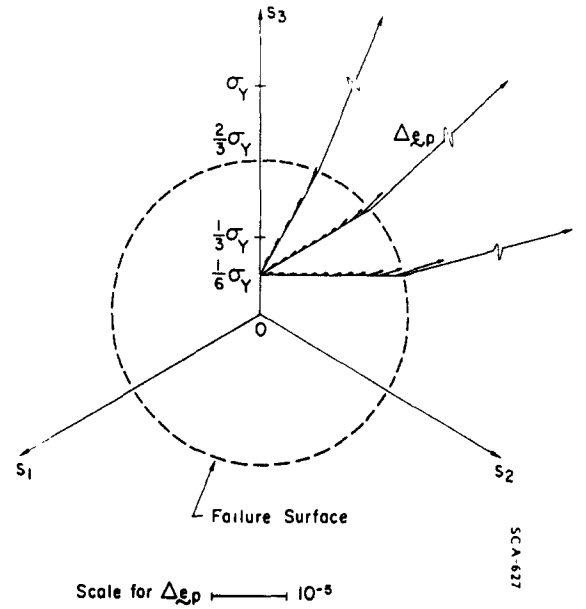

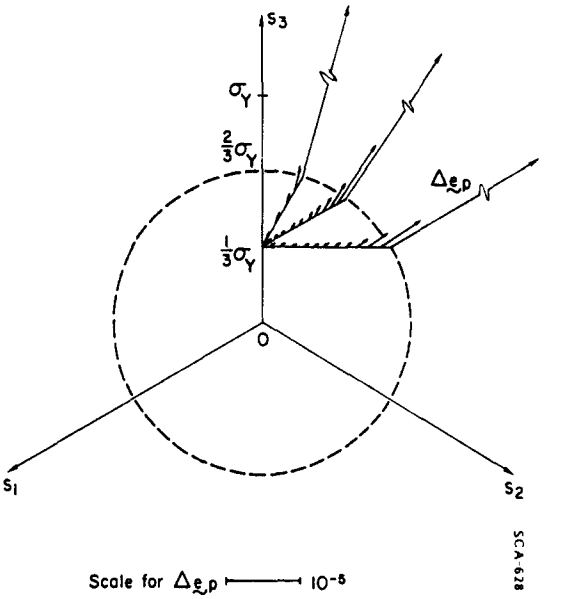

Fig. 7. Bilinear stress paths with corresponding plastic strain increment vectors predicted by the model: (a) radial loading to $\sigma_y/6$, (b) radial loading to $\sigma_y/3$.

plastic flow. Conversely, whenever this angle is equal to, or greater than, $\pi/2$, the model predicts purely elastic response, but only for infinitesimal stress increments in the new direction. For finite increments, the model leads to plastic flow for all changes in loading direction, a feature which provides the model with the ability to describe hysteresis under cyclic loading.

5. The response of the model to a number of complex (non-proportional) stress and strain paths was investigated numerically, using a simple explicit numerical scheme for incrementally integrating the governing system of equations. In all cases, the results from the numerical study were fully consistent with the analytical results derived herein, including the limiting cases of Section 4 and the asymptotic analysis of Section 5.

6. Proofs were given to show that the model obeys the postulates of (a) Stability in the Small[19] and (b) Isotropy[16].

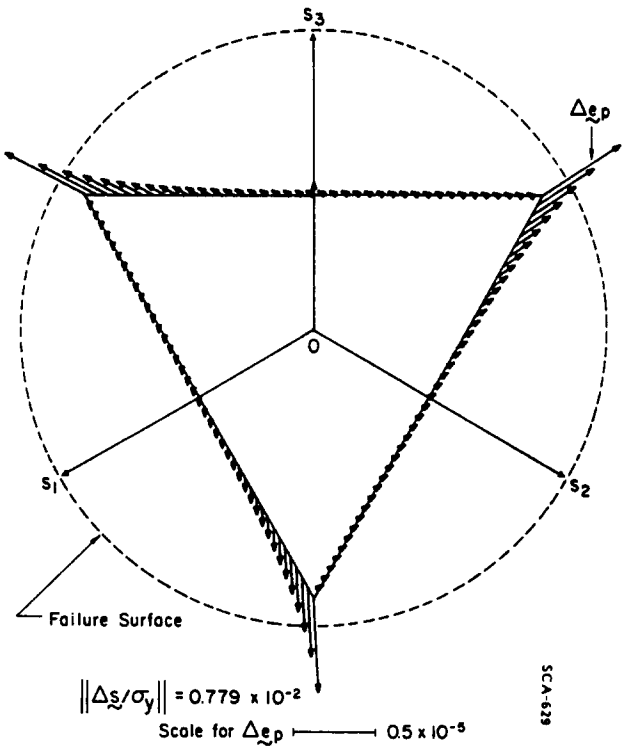

Fig. 8. Triangular stress path with corresponding plastic strain increment vectors predicted by the model.

The results from this study clearly demonstrate that the plastic flow properties of the new endochronic theory differ in significant and fundamental ways from those of classical plasticity.

Acknowledgement—This research was supported by the Air Force Office of Scientific Research (AFSC) under Contract F49620-84-C-0029.

REFERENCES

1. K. C. Valanis, A theory of viscoplasticity without a yield surface—part I: general theory. *Arch. Mech.* **23**, 517 (1971).
2. K. C. Valanis, A theory of viscoplasticity without a yield surface—part II: application to the mechanical behavior of metals. *Arch. Mech.* **23**, 535 (1971).
3. K. C. Valanis, Endochronic theory with proper hysteresis loop closure properties. S-CUBED (formerly Systems, Science and Software), La Jolla, California, Rep. SSS-R-80-4182, August (1979).
4. K. C. Valanis and C. F. Lee, Endochronic plasticity: physical basis and applications. *Proc. Intl. Confr. Constitutive Laws for Engr. Maths, Theory and Applications* (Edited by C. S. Desai). Tucson, Arizona (1983).
5. K. C. Valanis and J. Fan, Endochronic analysis of cyclic elastoplastic strain fields in a notched plate. *J. Appl. Mech.* **50**, 789 (1983).
6. K. C. Valanis and H. E. Read, A new endochronic plasticity model for soils. In *Soil Mechanics—Transient and Cyclic Loads* (Edited by G. N. Pande and O. C. Zienkiewicz). John Wiley, New York (1982).
7. K. C. Valanis and H. E. Read, An endochronic plasticity theory for concrete. *Mech. Mat.* (1986).
8. J. A. Trangenstein and H. E. Read, The inelastic response characteristics of the new endochronic theory with singular kernel. *Int. J. Solids Structures* **18**, 947 (1982).
9. Z. P. Bazant, R. J. Krizek and C.-L. Shieh, Hysteretic endochronic theory for sand. *J. Engng Mech. Div. ASCE* **109**(4), 1073 (1983).
10. H. E. Read, Discussion of hysteretic endochronic theory for sand. *J. Engng Mech. Div. ASCE* **111**(1), 103 (1985).
11. A. E. Taylor, *Advanced Calculus*. Ginn and Company, New York (1955).
12. G. F. Carrier, M. Krook and C. E. Pearson, *Functions of a Complex Variable, Theory and Technique*. McGraw-Hill, New York (1966).
13. K. C. Valanis, Private communication, April (1980).
14. Y. Ohashi, M. Tokuda and H. Yamashita, Effect of third invariant of stress deviator on plastic deformation of mild steel. *J. Mech. Phys. Solids* **23**, 295 (1975).

15. Y. Ohashi, T. Kurita, T. Suzuki and M. Tokuda, Experimental examination of the hypothesis of local determinability in the plastic deformation of metals. *J. Mech. Phys. Solids* **29**, 51 (1981).
16. A. A. Il'yushin, On the relation between stresses and small deformations in the mechanics of continuous media. *Prikl. Mat. Mekh.* **19**, 641 (1954).
17. V. S. Lenskii, Analysis of plastic behavior of metals under complex loading. *Plasticity, Proc. Second Symp. on Naval Structural Mechanics* (Edited by E. H. Lee and P. S. Symonds), p. 259. Pergamon Press, New York (1960).
18. D. D. Ivlev, On the postulate of isotropy in the theory of plasticity. *Izvestiya, Acad. Sci. USSR, Otd. Tekh. Nauk, ser. Mekh, i Mash.* **2**, 125 (1960).
19. D. C. Drucker, A definition of stable inelastic materials. *J. Appl. Mech.* **26**, 101 (1959).
20. W. Rudin, *Principles of Mathematical Analysis*, 3rd edn, p. 70. McGraw-Hill, New York (1964).

APPENDIX

1. *Postulate of isotropy*

The postulate of isotropy was introduced by Il'yushin[16] and further elaborated upon by Lenskii[17]. It asserts that if two strain histories are so related that the strain trajectory of one can be obtained from the strain trajectory of the other by a rotation or reflection in the strain space, then the stress history for one can be obtained from the stress history of the other by the same geometric transformation. Ivlev[18] also pointed out that the isotropy of the material (or model) does not necessarily imply that the postulate of isotropy will hold. In that which follows, a proof is given which shows that the new endochronic theory considered here satisfies the postulate of isotropy.

Consider the Laplace transform of ξ with respect to z:

$$\xi^* = \mathscr{L}(\xi) = \int_0^\infty \xi(z) e^{-\rho z}\, dz. \tag{A-1}$$

From eqn (1) and $\xi_\rho = 0$, at $z = 0$, one obtains

$$\xi^* = \rho^* p \varepsilon_\rho^* \tag{A-2}$$

where $\rho^* = \mathscr{L}(\rho)$.

Consider another pair (ξ'_ρ, ξ') which satisfies

$$\xi'_\rho = [R]\xi_\rho \tag{A-3}$$

where $[R]$ is an orthogonal matrix which is independent of z. Then

$$\xi'^* = \rho^* p \varepsilon'^*_\rho = p^* p [R] \xi_\rho^* = [R]\xi^* \tag{A-4}$$

which may be inverted to give

$$\xi' = [R]\xi, \tag{A-5}$$

thereby showing that the model satisfies the postulate of isotropy.

2. *Drucker's postulate*

The purpose of this section is to prove that the version of the new endochronic model treated herein satisfies the condition:

$$\varrho(z) \cdot \frac{d}{dz}\xi(z) \geqslant 0 \tag{B-1}$$

which is equivalent to Drucker's postulate of stability in the small[19].

Assume that

$$\rho(z) \equiv \rho_0 \frac{e^{-\beta z}}{z^\alpha} = \sum_{r=1}^{\infty} R_r e^{-\beta_r z} \qquad \text{for} \qquad \varepsilon < z \tag{B-2}$$

where $\varepsilon \ll 1$, $R_r > 0$, $\beta_r > 0$, and the series is uniformly convergent. The series is ordered in such a way that

$$\lim_{r \to \infty} e^{-\beta_r \varepsilon} = 0. \tag{B-3}$$

For $0 < z < \varepsilon \ll 1$, eqn (22) indicates that

$$\varrho(z) \cdot \frac{d}{dz}\xi(z) = \rho(z) > 0. \tag{B-4}$$

For $\varepsilon < z < \infty$, eqn (17) yields

$$\underset{\sim}{q}(z)\cdot\frac{\mathrm{d}}{\mathrm{d}z}\underset{\sim}{\xi}(z)=\rho(\varepsilon)\underset{\sim}{q}(z)\cdot\underset{\sim}{q}(z-\varepsilon)+\int_0^{\varepsilon}\rho(y)\underset{\sim}{q}(z)\cdot\frac{\mathrm{d}\underset{\sim}{q}(z-y)}{\mathrm{d}z}\,\mathrm{d}y+\int_{\varepsilon}^{z}\frac{\mathrm{d}\rho(y)}{\mathrm{d}y}\underset{\sim}{q}(z)\cdot\underset{\sim}{q}(z-y)\,\mathrm{d}y. \tag{B-5}$$

The right-hand side terms can be expanded as follows:

$$\begin{aligned}\rho(\varepsilon)\underset{\sim}{q}(z)\cdot\underset{\sim}{q}(z-\varepsilon)&=\rho(\varepsilon)\underset{\sim}{q}(z)\cdot\left[\underset{\sim}{q}(z)-\varepsilon\underset{\sim}{q}'(z)+\frac{\varepsilon^2}{2}\underset{\sim}{q}''(z)-\cdots\right]\\&=\rho(\varepsilon)\left[1+\frac{\varepsilon^2}{2}\,\underset{\sim}{q}(z)\cdot\underset{\sim}{q}''(z)+0(\varepsilon^3)\right]\end{aligned} \tag{B-6}$$

$$\begin{aligned}\int_0^{\varepsilon}\rho(y)\underset{\sim}{q}(z)\cdot\frac{\mathrm{d}\underset{\sim}{q}(z-y)}{\mathrm{d}z}\,\mathrm{d}y&=\int_0^{\varepsilon}\rho(y)\underset{\sim}{q}(z)\cdot[\underset{\sim}{q}'(z)-y\underset{\sim}{q}''(z)+\cdots]\,\mathrm{d}y\\&=-\underset{\sim}{q}(z)\cdot\underset{\sim}{q}''(z)\frac{\rho_0\varepsilon^{2-\alpha}}{2-\alpha}+0(\varepsilon^{3-\alpha}).\end{aligned} \tag{B-7}$$

Since the series (B-2) is uniformly convergent and the derivative of the series is also uniformly convergent, as shown in the sequel, it is possible to write

$$\frac{\mathrm{d}\rho(y)}{\mathrm{d}y}=-\sum_{r=1}^{\infty}\beta_r R_r e^{-\beta_r y}\qquad\text{for}\qquad \varepsilon<z<\infty. \tag{B-8}$$

Since $\sum_{r=1}^{\infty}\frac{R_r}{\beta_r}$ is convergent, as shown in eqn (57b), and $\lim_{r\to\infty}\beta_r^2 e^{-\beta_r y}=0$ due to eqn (B-2), the series in eqn (B-8) is uniformly convergent by virtue of the theorem for the convergence of the series consisting of the products of two sequences; see for instance, Ref. [20], p. 70. The use of eqn (B-7) with $|\underset{\sim}{q}(z)\cdot\underset{\sim}{q}(z-y)|\leqslant 1$ yields

$$\left|\int_{\varepsilon}^{z}\frac{\mathrm{d}\rho(y)}{\mathrm{d}y}\underset{\sim}{q}(z)\cdot\underset{\sim}{q}(z-y)\,\mathrm{d}y\right|\leqslant\rho(\varepsilon)-\rho(z). \tag{B-9}$$

Equation (B-5) with eqns (B-6), (B-7) and (B-9) yields eqn (B-1). Noting that $\underset{\sim}{l}\equiv\mathrm{d}\underset{\sim}{\xi}/\|\mathrm{d}\underset{\sim}{\xi}\|$, it follows from eqn (B-1) that

$$\cos\theta\equiv\underset{\sim}{a}\cdot\underset{\sim}{l}>0. \tag{B-10}$$